Archival Report

Biological Psychiatry: CNNI

Dynamic Functional Hyperconnectivity After Psilocybin Intake Is Primarily Associated With Oceanic Boundlessness

Sepehr Mortaheb, Larry D. Fort, Natasha L. Mason, Pablo Mallaroni, Johannes G. Ramaekers, and Athena Demertzi

ABSTRACT

BACKGROUND: Psilocybin is a widely studied psychedelic substance that leads to the psychedelic state, a specific altered state of consciousness. To date, the relationship between the psychedelic state's neurobiological and experiential patterns remains undercharacterized because they are often analyzed separately. We investigated the relationship between neurobiological and experiential patterns after psilocybin by focusing on the link between dynamic cerebral connectivity and retrospective questionnaire assessment.

METHODS: Healthy participants were randomized to receive either psilocybin (n = 22) or placebo (n = 27) and scanned for 6 minutes in an eyes-open resting state during the peak subjective drug effect (102 minutes posttreatment) in ultrahigh field 7T magnetic resonance imaging. The 5-Dimensional Altered States of Consciousness Rating Scale was administered 360 minutes after drug intake.

RESULTS: Under psilocybin, there were alterations across all dimensions of the 5-Dimensional Altered States of Consciousness Rating Scale and widespread increases in averaged brain functional connectivity. Time-varying functional connectivity analysis unveiled a recurrent hyperconnected pattern characterized by low blood oxygen level–dependent signal amplitude, suggesting heightened cortical arousal. In terms of neuroexperiential links, canonical correlation analysis showed higher transition probabilities to the hyperconnected pattern with feelings of oceanic boundlessness and secondly with visionary restructuralization.

CONCLUSIONS: Psilocybin generates profound alterations at both the brain and the experiential levels. We suggest that the brain's tendency to enter a hyperconnected-hyperarousal pattern under psilocybin represents the potential to entertain variant mental associations. These findings illuminate the intricate interplay between brain dynamics and subjective experience under psilocybin, thereby providing insights into the neurophysiology and neuroexperiential qualities of the psychedelic state.

https://doi.org/10.1016/j.bpsc.2024.04.001

Hallucinogens are psychoactive drugs that, historically, have been used to alter conscious experience (1,2). These drugs are divided into the classes of serotonergic psychedelics (e.g., psilocybin), antiglutamatergic dissociatives (e.g., ketamine), anticholinergic deliriants (e.g., scopolamine), and kappa opioid agonists (e.g., salvinorin A) (3). Research on classical hallucinogens has focused largely on serotonergic psychedelics, such as lysergic acid diethylamide (LSD), ayahuasca, psilocybin, *N,N*-dimethyltryptamine (DMT), and mescaline (4). Among them, psilocybin has been one of the most studied psychedelics, possibly due to its potential contribution to treating different disorders (5), such as obsessive-compulsive disorder (6), death-related anxiety (7), depression (8–11), treatment-resistant depression (12–14), major depressive disorder (15), terminal cancer–associated anxiety (11,16), demoralization (17), smoking (18), and alcohol and tobacco addiction (19–21).

The acute phase of psilocybin administration leads to the psychedelic state, which is a specific altered state of consciousness associated with consuming psilocybin and LSD (22). By "state" we refer to the combination of neurobiological and experiential patterns that are associated with the psychedelic experience (23). In terms of general experiential alterations, the psychedelic state has been associated with ego dissolution, i.e., a reduction in self-referential awareness, which ultimately disrupts self-world boundaries with increasing feelings of unity with others and one's own surroundings (24–26), unconstrained and hyperassociative cognition (27,28), profound alterations in the perception of time and space (29,30), perceptual alterations, synesthesia, amplification of emotional state (31), and emotional volatility (32). Long-term and enduring effects on personality and mood have also been reported, such as increases in openness and extraversion, decreases in neuroticism, and increases in mindful awareness (33–35). In terms of the neurobiological pattern, psilocybin administration has been shown to result in increased cerebral connectivity with reduced modularity,

ISSN: 2451-9022

whether in the acute or postacute phase (36–38). Regionwise, there have been reports of decreased activity in the thalamus, posterior cingulate cortex, and medial prefrontal cortex (10) and altered connectivity of the claustrum (39). Networkwise, decreased connectivity has been reported within the default mode network (DMN) (1,10), visual network (1), and executive control network (40), as well as reduced segregation of the dorsal attentional network and executive control network (41). These neural counterparts indicate that the subjective effects of psilocybin are linked to alterations in the activity and connectivity of important brain regions involved in information integration and routing when averaged signal analysis is concerned. Dynamic analyses of connectivity patterns after psilocybin administration have shown that the brain tended to recurrently configure into transient functional patterns with low stability (42). In addition, under psilocybin, there were higher probabilities for the brain to configure into a connectivity pattern characterized by global cortex-wide positive phase coherence (43). In terms of state transition dynamics, a recent study calculated the minimum network control energy required to transition between states (or maintain the same state) and found that the network control energy landscape was flattened under LSD and psilocybin, meaning that there were more frequent state transitions and increased entropy of brain pattern dynamics (44). Taken together, averaged and dynamic connectivity analyses suggest that psilocybin alters brain function such that the overall neurobiological pattern becomes functionally more connected, more fluid, and less modular.

The link between the brain's functional dynamic reconfigurations and the psychedelic state's experiential patterns is notable. A recent investigation correlated the occurrence rates of prominent connectivity patterns (i.e., frontoparietal subsystem and a globally coherent pattern) with subjective drug intensity measured on a 10-point Likert scale (43,45). Although this approach has provided insights into the ensuing psychedelic state, it can be argued that, due to its simplicity, subjective drug intensity cannot capture the complexity of the psychedelic state's phenomenological pattern. Here, we adopted a neuroexperiential approach, which we define as the quantification and comparison of both the neurobiological and experiential patterns. This approach allows the investigation of psilocybin's effects on cerebral functional dynamics and the linking of these dynamic spatiotemporal fingerprints with reported experiential alterations measured retrospectively with standardized assessment.

METHODS AND MATERIALS

This study was conducted according to the code of ethics on human experimentation established by the Declaration of Helsinki (1964) and amended in Fortaleza (Brazil, October 2013). This study was in accordance with the Medical Research Involving Human Subjects Act and was approved by the Academic Hospital and the University's Medical Ethics Committee (Maastricht University, Netherlands Trial Register: NTR6505). All participants were fully informed of all procedures, possible adverse reactions, legal rights, responsibilities, expected benefits, and their right to voluntary termination without consequences.

Participants

In the current study, we analyzed previously collected data on 49 healthy participants with previous experience with a psychedelic drug but not within the past 3 months of the experiment (1). Participants were randomized to receive a single dose of psilocybin (0.17 mg/kg, n = 22; 12 male; age, mean ± SD = 23 ± 2.9 years) or placebo (n = 27; 15 male; age = 23.1 ± 3.8 years).

Procedure

Participants were familiarized with the test day procedures on a separate training day prior to the treatment conditions. Participants were instructed to refrain from drug use, including use of psychedelic drugs (≥3 months), MDMA/ecstasy (≥14 days), alcohol (≥24 hours), and all other drugs of abuse (≥7 days) prior to their test day. Additionally, participants were asked to refrain from caffeine and nicotine use on the test day. On test days, the absence of drug and alcohol use were assessed via a urine drug screen and a breath alcohol screen. An additional pregnancy test was given if participants were female. If all tests were found to be negative, participants were allowed to proceed. After measurements, the treatment was administered orally in a closed cup containing bitter lemon (placebo) or bitter lemon and psilocybin (powder). After 40 minutes, participants were placed in the magnetic resonance imaging (MRI) scanner, where resting-state scans and magnetic resonance spectroscopy were performed throughout a 1-hour time window. Six minutes of resting-state functional MRI (fMRI) were acquired from the participants with eyes open. At the end of the test day (approximately 6 hours after treatment administration), participants were asked to complete measures of retrospective subjective experience (5-Dimensional Altered States of Consciousness Rating Scale [5D-ASC]). Participants stayed under supervision until the testing day was complete, and the researcher deemed them fit to go home.

Phenomenological Assessment

The 5D-ASC is a 94-item self-report scale that assesses participants' subjective experiences after an altered state of consciousness and as such is termed a retrospective phenomenological assessment (46,47). On this questionnaire, participants are asked to make a vertical mark on the 10-cm line below each statement to rate the extent to which the following statements apply to their experience: "No, not more than usual" to "Yes, more than usual." The 5D-ASC comprises 5 dimensions, including oceanic boundlessness (OBN), dread of ego dissolution, visionary restructuralization (VRS), auditory alterations, and vigilance reduction. Furthermore, OBN, dread of ego dissolution, and VRS can be organized into 11 subscales via a previously published factor analysis (25) comprising the 11 factors of the ASC (11-ASC) scoring scheme. OBN includes experience of unity, spiritual experience, blissful state, insightfulness, and disembodiment; dread of ego dissolution includes impaired control and cognition and anxiety; and VRS includes complex imagery, elementary imagery, audio-visual synesthesia, and changed meaning of percepts.

Analysis encompassed an initial assessment for normality assumptions of the 5D-ASC and its 11-ASC factors using the Shapiro-Wilk tests set at α = 0.05. In case of violations of

normality, nonparametric Mann-Whitney *U* tests were used to compare the 5D-ASC and 11-ASC scores in the 2 groups. *p* Values were corrected using the Bonferroni method, with the significance level set at $\alpha = 0.05$. The effect size was calculated based on the glass rank biserial coefficient.

Neuroimaging Setup and Analysis

Images were acquired on a 7T Siemens MAGNETOM scanner (Siemens Medical) using a 32 receiving channel head array Nova coil (NOVA Medical Inc.). The T1-weighted images were acquired using a magnetization-prepared 2 rapid acquisition gradient-echo sequence collecting 190 sagittal slices with the following parameters: repetition time = 4500 ms, echo time = 2.39 ms, inversion times TI1/TI2 = 900/2750 ms, flip angle 1 = 5°, flip angle 2 = 3°, voxel size = 0.9 mm isotropic, bandwidth = 250 Hz/pixel. In addition, 258 whole-brain echo-planar image volumes were acquired at rest (repetition time = 1400 ms, echo time = 21 ms, field of view = 198 mm^2, flip angle = 60°, oblique acquisition orientation, interleaved slice acquisition, 72 slices, slice thickness = 1.5 mm, voxel size = 1.5 × 1.5 × 1.5 mm^3).

Preprocessing. fMRI data were preprocessed using a local pipeline based on SPM12 (48) and FSL 6.0.4 (49). After realignment and susceptibility distortion correction [FSL topup (50)], functional data were registered to the high-resolution T1 image, then normalized to the standard Montreal Neurological Institute space, and finally smoothed using a Gaussian kernel with a full width at half maximum of 6 mm. After segmentation of the structural T1 image into gray matter, white matter, and cerebrospinal fluid masks, the bias-corrected structural image and all the extracted masks were normalized to the Montreal Neurological Institute space. Furthermore, white matter and cerebrospinal fluid masks were eroded by 1 voxel to remove any overlap between these tissues and the gray matter voxels. To denoise functional time series, we used a locally developed pipeline written in Python [nipype package (51)]. In this pipeline, a general linear model was fitted to each voxel data separately, regressing out the effect of 6 movement parameters (translation in x, y, and z directions and rotation in yaw, roll, and pitch directions) and their first derivative, constant and linear trends using zero-order and first-order Legendre polynomials, and 5 principal components of signals in the white matter and cerebrospinal fluid masks. In addition, outlier detection was performed using the ART toolbox (http://web.mit.edu/swg/software.htm), and outliers were modeled as nuisance regressors in the general linear model. Any volume with a movement value of >3 mm, rotation value of >0.05 radians, and *z*-normalized global signal intensity of >3 was considered an outlier. After regressing out these nuisance regressors, the remaining signal was filtered in the range of 0.008–0.09 Hz and was used for further analysis. The Schaefer atlas with 100 regions of interest (ROIs) and a resolution of 2 mm (52) were used to extract the averaged blood oxygen level–dependent (BOLD) signals inside each ROI.

Estimation of Averaged Functional Connectivity. Pearson correlations were calculated between the BOLD time series for every pair of ROIs and subsequently Fisher-transformed, which resulted in the generation of a 100 × 100 connectivity matrix for each participant. An independent *t* test was used to compare the 4950 possible between-region connectivity values between the 2 groups. False discovery rate (FDR) correction was performed to correct for multiple comparisons. Furthermore, the average of the connectivity values over the whole brain was calculated for each participant and was considered as the overall connectivity value of the brain. An independent *t* test was performed to compare the overall connectivity values in the psilocybin and placebo groups.

Estimation of Time-Varying Functional Connectivity. We used phase-based coherence to extract between-region connectivity patterns at each time point of the scanning session (52,53). For each participant *i*, after *z*-normalization of time series at each region *r* (i.e., $x_{i,r}[t]$), the instantaneous phase of each time series was calculated via Hilbert transform as:

$$\widehat{x}_{i,r}(t) = \frac{1}{\pi t} * x_{i,r}(t) \tag{1}$$

where $*$ indicates a convolution operator. Using this transformation, we produced an analytical signal for each regional time series as:

$$x^a_{i,r}(t) = x_{i,r}(t) + j\widehat{x}_{i,r}(t) \tag{2}$$

where $j = \sqrt{-1}$. From this analytical signal, the instantaneous phase of each time series can be estimated as:

$$\varphi_{i,r}(t) = \tan^{-1}\left(\frac{\widehat{x}_{i,r}(t)}{x_{i,r}(t)}\right) \tag{3}$$

After wrapping each instantaneous phase signal of $\varphi_{i,r}(t)$ to the $[-\pi, \pi]$ interval and naming the obtained signal as $\theta_{i,r}(t)$, we calculated a connectivity measure for each pair of regions as the cosine of their phase difference. For example, the connectivity measure between regions *r* and *s* in participant *i* was defined as:

$$conn_{i,r,s}(t) \triangleq \cos\left(\theta_{i,r}(t) - \theta_{i,s}(t)\right) \tag{4}$$

By this definition, completely synchronized time series lead to a connectivity value of 1, completely desynchronized time series produce a connectivity value of 0, and anticorrelated time series produce a connectivity measure of −1. Using this approach, we created a connectivity matrix of 100 × 100 at each time point *t* for each participant *i* that we called $C_i(t)$:

$$C_i(t) \triangleq \left[conn_{i,r,s}(t)\right]_{r,s} \tag{5}$$

After collecting the connectivity matrices across all time points and participants, *k*-means clustering was applied, with 500 repetitions and 200 iterations at each repetition. With this technique, 4 robust and reproducible patterns were extracted as the centroids of the clusters, and each resting connectivity matrix was assigned to one of the extracted patterns. To be comprehensive, we performed supplementary analyses by varying the number of clusters $k = 3$–7 (Figure S3).

We calculated the occurrence rate of each pattern defined as the proportion of connectivity matrices assigned to that pattern for each participant separately. Independent 2-tailed

t tests were used to compare the occurrence rate of each functional connectivity (FC) pattern in the psychedelic and placebo groups. Bonferroni correction was used to correct the p values for multiple comparisons across the 4 connectivity patterns.

Dynamic State Transition Modeling. To investigate the temporal evolution of the identified connectivity matrices, we defined the extracted patterns as the distinct states of a dynamic system, transitioning between them over time using Markov modeling (53). Using this approach, the data of a sample participant could be stated as a sequence of connectivity patterns over time (i.e., $\{P_t \mid t : 1, \ldots, T \text{ and } P_t \in \{1, \ldots, M\}\}$, where M is the number of patterns and T is the number of signal time points). In this case, the probability of transitioning from pattern I to pattern J defined as $p(I \rightarrow J)$, considering $I, J \in \{1, .., M\}$, can be calculated as the number of consecutive I, J pairs in the sequence divided by the total number of transitions from pattern I:

$$p(I \rightarrow J) = \frac{\sum_{t=0}^{T-1} [(P_t == I) \,\&\, (P_{t+1} == J)]}{\sum_{j=1}^{M} \sum_{t=0}^{T-1} [(P_t == I) \,\&\, (P_{t+1} == j)]} \quad (6)$$

This transition probability was estimated for each possible between-state transition and each participant separately. With this approach, we could compare any significant difference in transition probabilities between 2 groups of participants. To detect significantly different transition probabilities between the 2 groups, a Wilcoxon rank-sum test was performed on each transition, and p values were FDR corrected.

Regional BOLD Amplitude Analysis. The Euclidean norm of the BOLD signal was calculated at each ROI as a measure of the power of the signal. Independent t tests were used to compare the regional BOLD signal power between the 2 groups, and p values were FDR corrected due to multiple comparisons.

Neuroexperiential Analysis. A canonical correlation analysis (CCA) was conducted using the 16 dynamic patterns transition probability variables as features of the neuronal space and the 11-ASC variables as features of the phenomenological space to evaluate the multivariate shared relationship between the 2 variable sets. CCA is a multivariate latent variable model that identifies associations between 2 different data modalities (54). Considering matrix $X^{N \times M}$ contains M neuronal features of N participants, and $Y^{N \times P}$ contains P questionnaire features of N participants, the objective of the CCA is to find pairs of neuronal and questionnaire weights $w_x^{M \times 1}$ and $w_y^{P \times 1}$ such that the weighted sum of the neuronal and experiential variables maximizes the correlation between the resulting latent variables (canonical variates):

$$\max_{w_x, w_y} corr(Xw_x, Yw_y) \quad (7)$$

After finding the latent variables Xw_x and Yw_y that have the maximal correlation, the features in each data modality that have a stronger correlation with their respective latent variable are also significantly associated with one another. To account for overfitting, we used a permutation test to calculate the significance of correlation values. This was achieved by random shuffling of observations in the neural space compared with the observations in the phenomenological space. The procedure was repeated 100,000 times, and at each iteration, a CCA model was fitted to the data, and the correlation values were calculated. These values were used to construct the null distribution and to calculate the p value of the observed correlation value in the main analysis. The obtained p values were FDR corrected to account for the multiple comparisons.

Validation of the Results. We analyzed the potential effects of motion, atlas parcellation, and global signal regression on the main results. To quantify motion, we calculated the mean framewise displacement (FD) (55,56) for each participant as well as for each time-varying connectivity pattern. Independent t tests were used to compare the mean FD between the placebo and psilocybin groups as well as between time-varying connectivity patterns. Furthermore, the Pearson correlation between the mean FD and either mean FC or mean BOLD signal amplitude was calculated. To investigate the role of subcortical regions, we incorporated 19 subcortical regions (the brainstem together with the thalamus, caudate, putamen, pallidum, hippocampus, amygdala, accumbens area, ventral diencephalon, and cerebellum in the right and left hemispheres) sourced from the Human Connectome Project (57–59) into the initially utilized Schaefer atlas, which resulted in an atlas with 119 ROIs. Next, we performed both averaged and dynamic FC analyses using this combined atlas. Finally, to verify the effect of the global signal on the analysis results, we also performed all the analyses after global signal regression.

RESULTS

Experiential Assessment

All variables of the 5D-ASC and its 11-ASC factors violated the assumption of normality (Table S1). As a result, Mann-Whitney U tests were used to compare the phenomenological outcomes in the 2 groups. Analyses revealed significant differences in all dimensions and factors with large effect sizes, such that the psilocybin group had more substantial effects than the placebo (Figure 1A, B and Table 1).

Neuroimaging

After psilocybin, whole-brain averaged connectivity increased (independent t test: $t_{47} = 3.087$, $p = .004$) (Figure 2A). This overall increase was further observed as a cortex-wide increase in the connectivity matrix values (independent t test on the between-region connectivity values with FDR correction) (Figure 2B) and an increase in the averaged connectivity values in the transmodal regions (independent t test on the regional averaged connectivity values with FDR correction) (Figure S1). These alterations in the connectivity values were also accompanied by changes in the BOLD signal amplitude. By calculating the Euclidean norm of the BOLD time series related to each ROI, we found that regional BOLD signal amplitude decreased after psilocybin administration in both posterior and anterior regions compared with the placebo group

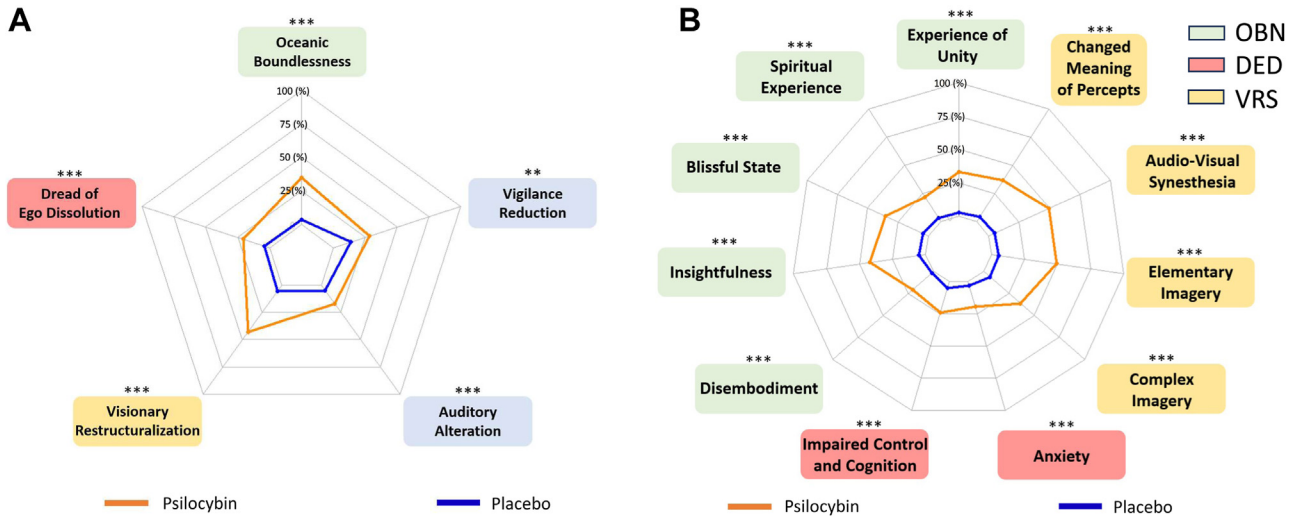

Figure 1. Substantial alterations in subjective experience were reported after psilocybin administration compared to placebo. **(A)** The assessment of 5-Dimensional Altered States of Consciousness Rating Scale showed that the administration of psilocybin significantly altered subjective experience in all dimensions. **(B)** The same effect was also observed considering the 11 factors of altered states of consciousness. Radar plots illustrate group means for each dimension/factor. $^{**}p < .005$, $^{***}p < .001$. DED, dread of ego dissolution; OBN, oceanic boundlessness; VRS, visionary restructuralization.

(independent *t* test, FDR corrected) (Figure 2C and Figure S2). While somatomotor, limbic network, and temporal regions of the DMN did not show significant changes in their signal norm, the highest decrease in BOLD signal amplitude was related to the posterior cingulate cortex and parietal regions of the external control network.

Time-varying analysis revealed variant and distinct patterns of complex interareal interactions: one of both correlations and anticorrelations (pattern 1), one of anticorrelations of the DMN with other networks (pattern 2), one of global cortex-wide positive connectivity (pattern 3), and one of low interareal connectivity (pattern 4). Pattern 3 occurred significantly more often in the psilocybin group than in the placebo group (independent *t* test: $t_{47} = 3.731$, $p = .001$, $\alpha_{Bonferroni} = 0.05/4 = 0.0125$) (Figure 2D). Supplementary analyses using $k = 3$–7 clusters showed that the same connectivity patterns were replicable, and hyperconnectivity had a higher occurrence rate in the psychedelic state (Figure S3). In terms of dynamic transitions, the psilocybin group showed significantly higher transition probabilities toward pattern 3 from pattern 1 (Wilcoxon rank-sum test: $z = 2.744$, $p = .006$), pattern 3 ($z = 2.291$, $p = .022$), and pattern 4 ($z = 2.000$, $p = .045$) (Figure 2E).

Table 1. Substantial Changes in Subjective Experience After Psilocybin Administration Compared With Placebo

Scale	Subjective Experience	Psilocybin, *n* = 21, Mean (SD)	Placebo, *n* = 26, Mean (SD)	Statistics, Mann-Whitney *U* Test		
				U	rg	*p*
5D-ASC	Oceanic boundlessness	35.09 (23.58)	3.78 (5.56)	528.5	0.936	<.001
	Dread of ego dissolution	20.54 (17.12)	3.94 (8.05)	494	0.81	<.001
	Visionary restructuralization	42.97 (19.20)	5.33 (9.23)	528.5	0.936	<.01
	Auditory alterations	16.99 (17.18)	4.69 (12.97)	458.5	0.679	<.001
	Vigilance reduction	28.18 (20.43)	13.99 (16.33)	400.5	0.467	<.001
11-ASC	Insightfulness	42.44 (29.77)	4.99 (7.39)	508	0.861	<.001
	Spiritual experience	21.73 (22.04)	3.33 (6.91)	435	0.593	<.001
	Experience of unity	33.27 (30.57)	2.85 (4.70)	483.5	0.771	<.001
	Blissful state	35.65 (27.02)	4.36 (7.04)	489	0.791	<.001
	Disembodiment	20.65 (25.71)	1.74 (1.82)	434	0.59	<.001
	Anxiety	19.55 (22.57)	3.01 (4.30)	430	0.575	<.001
	Impaired control and cognition	24.29 (18.35)	4.77 (12.51)	497	0.821	<.001
	Changed meaning of percept	36.75 (29.65)	4.24 (8.92)	495.5	0.815	<.001
	Audio-visual synesthesia	49.54 (22.82)	4.94 (12.99)	525	0.923	<.001
	Complex imagery	36.43 (25.49)	6.22 (12.03)	528.5	0.839	<.001
	Elementary imagery	49.25 (21.95)	5.68 (9.24)	502	0.943	<.001

5D-ASC, 5-Dimensional Altered States of Consciousness Rating Scale; 11-ASC, 11 factors of ASC sorting scheme; rg, glass rank biserial coefficient effect size.

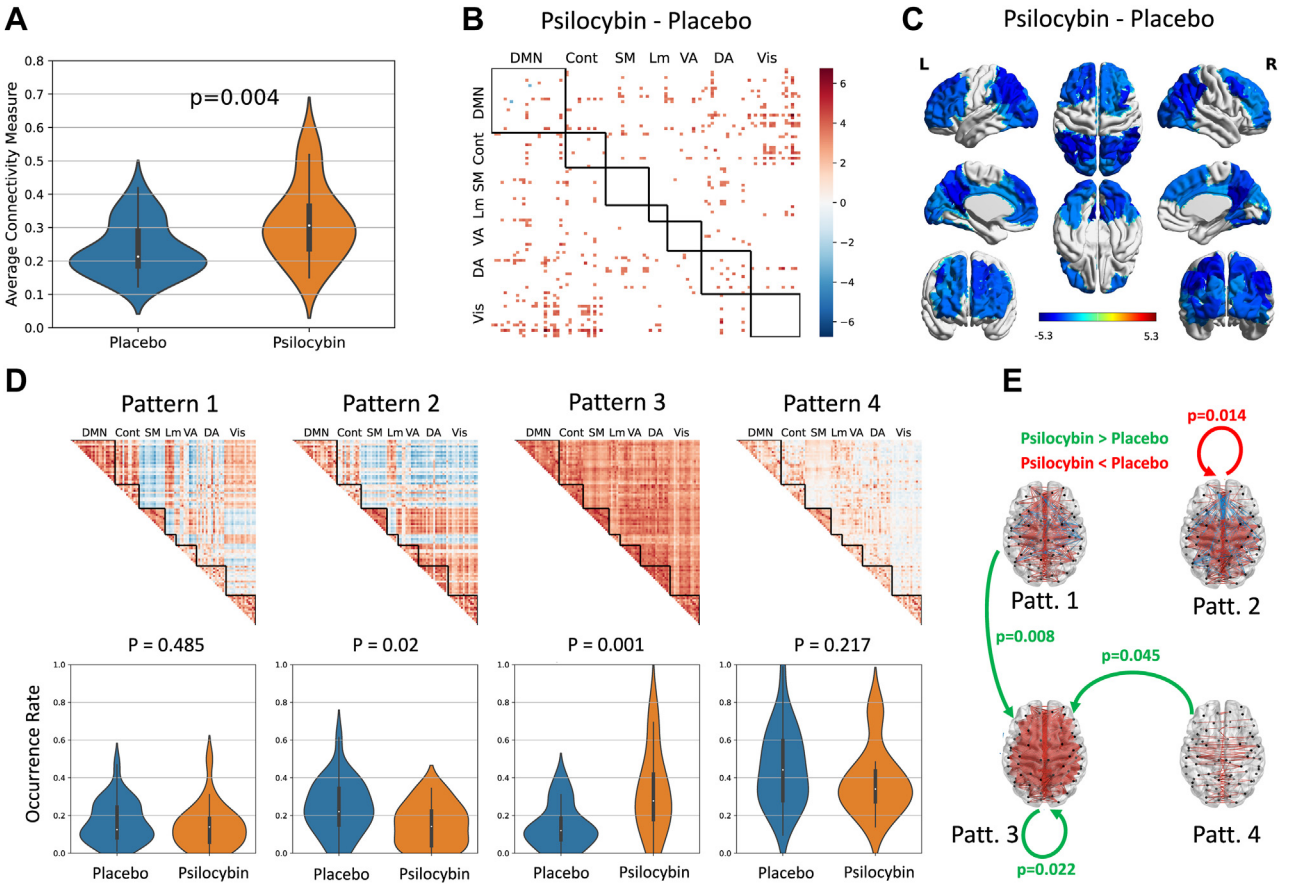

Figure 2. After psilocybin administration, there was an overall cerebral tendency to show more reoccurrence of a functional hyperconnectivity pattern. **(A)** Averaged functional connectivity expressed as Fisher-transformed correlation values increased significantly after psilocybin administration compared with the placebo group. **(B)** There were higher interregional connectivity values in the psilocybin group. The matrix represents *t* values comparing the connectivity matrices of the psilocybin group and those of the placebo group (contrast: psilocybin minus placebo). Only significantly different values are colored. **(C)** The blood oxygen level–dependent amplitude of posterior and anterior brain regions decreased after psilocybin administration, while the amplitude of somatomotor and limbic areas, as well as the temporal regions of the default mode network (DMN), remain unchanged. Colors are based on *t* values comparing the Euclidean norm of blood oxygen level–dependent time series in the psilocybin group and the placebo group at each region of interest; only significantly different values are colored. **(D)** The functional connectome reconfigures in 4 connectivity patterns, ranging from complex interareal interactions (pattern 1) to a low interareal connectivity profile (pattern 4). After psilocybin administration, there was a significant increase in the occurrence rate of the global cortex-wide positive connectivity (pattern 3). The connectivity matrices are colored based on the connectivity value: from dark blue to dark red corresponds to connectivity values from −1 to +1. Violin plots represent the distribution of patterns' occurrence rates across participants. **(E)** The transition probability from other patterns to pattern 3 increased in the psilocybin group. Arrows indicate transitions between functional connectivity states. Green corresponds to significantly higher transition probabilities (Wilcoxon rank-sum test) for the psilocybin group than the placebo group, and red corresponds to significantly higher transition probabilities for the placebo group than the psilocybin group. Cont, executive control network; DA, dorsal attentional network; L, left; Lm, limbic network; Patt, pattern; R, right; SM, somatomotor network; VA, ventral attentional network; Vis, visual network.

In addition, the psilocybin group showed lower transition probabilities from pattern 2 to itself than the placebo group ($z = -2.452$, $p = .014$).

The neuroexperiential link was investigated with CCA, by which we estimated the first canonical vector for both the behavioral and neural spaces that maximized the shared correlation between the 2 spaces ($r = 0.97$, $p < .001$). Considering the neural space, the transition probabilities from pattern 1 to pattern 3 showed the highest correlation with the first canonical vector of the neural space ($r = 0.86$, $p < .001$) (Figure 3A). In addition, the transition from pattern 4 to pattern 3 ($r = 0.40$, $p = .016$) showed a lower significant correlation with the first canonical vector of the neural space. In the questionnaire space, factors related to OBN (experience of unity: $r = 0.80$, $p = .008$; blissful state: $r = 0.74$, $p = .010$; insightfulness: $r = 0.68$, $p = .013$; spiritual experience: $r = 0.62$, $p = .044$) and VRS (elementary imagery: $r = 0.67$, $p = .012$; audio-video synesthesia: $r = 0.61$, $p = .021$) showed the highest correlations with the first canonical vector of this space (Figure 3B). To account for overfitting, we used a permutation test to calculate the significance of correlation values. This was achieved by random shuffling of observations in the neural space compared with the observations in the questionnaire space. The procedure was repeated 100,000 times, and at each iteration, a CCA model was fitted to the data, and the correlation values were calculated. These values were used to construct

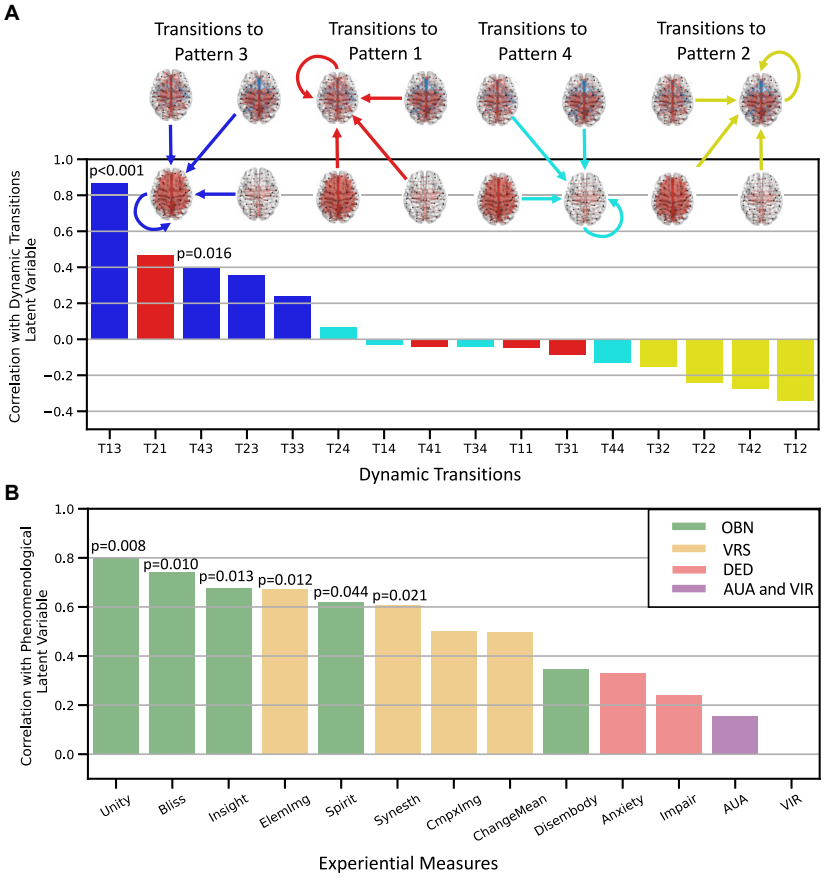

Figure 3. The neuroexperiential analysis indicated that transitions to the hyperconnected pattern 3 were linked to the factors of oceanic boundlessness (OBN) and visionary restructuralization (VRS). **(A)** In the neural space, the canonical correlation analysis showed that the transition probabilities to the hyperconnected pattern had the highest correlation with the first canonical vector of the space. Demonstrated *p* values are related to the significant correlation values and are false discovery rate corrected. The x-axis represents pattern transitions (T), e.g., T13: transition from pattern 1 to pattern 3. **(B)** In the phenomenological space, factors related to the dimension of OBN and VRS showed the highest correlation with the first canonical vector of the space. Bars represent correlation values of each factor to the first canonical vector of its associated space. AUA, auditory alterations; Bliss, blissful state; ChangeMean, changed meaning of percept; CmpxImg, complex imagery; DED, dread of ego dissolution; Disembody, disembodiment; ElemImg, elementary imagery; Impair, impaired control and cognition; Insight, insightfulness; Spirit, spiritual experience; Synesth, audio-visual synesthesia; Unity, experience of unity; VIR, vigilance reduction.

the null distribution and to calculate the *p* value of the observed correlation value in the main analysis. The obtained *p* values were FDR corrected to account for multiple comparisons. To validate the results, we also performed a CCA analysis between the dimensions of the 5D-ASC and the between-state transition probabilities. At the neural space, the transition probability from pattern 1 to pattern 3 showed the highest correlation with the first canonical vector of the neural space ($r = 0.89$, $p < .001$), and at the questionnaire space, OBN showed the highest correlation with the first canonical vector ($r = 0.93$, $p = .0145$) (Table 2).

Validation

The analysis of the effect of motion revealed comparable values in terms of mean FD between the psilocybin and placebo group (independent *t* test $t_{47} = -0.31$, $p = .76$) (Figure S4A), as well as between the connectivity patterns (Figure S4B). Additionally, no significant correlations were observed between mean FD and either mean FC values ($r = 0.23$, $p = .12$) or mean BOLD signal amplitude ($r = 0.11$, $p = .43$) (Figure S4C). Furthermore, the connectivity results were replicated even after adding subcortical regions to the parcellation atlas (Figure S5). However, regressing out the global signal led to the absence of a significant increase in FC values in the psilocybin group (Figure S6A, B), as well as the absence of a hyperconnectivity pattern in the dynamic functional analysis (Figure S6C), as was also shown previously (59). Given that the global signal (GS) amplitude was lower in the psilocybin group and that motion values were comparable in the psilocybin and placebo groups, we consider the possibility that GS may contain inherent information about the psychedelic state. Therefore, we opted to retain the GS in the main analyses.

DISCUSSION

We investigated the effect of the serotonergic hallucinogen psilocybin on the brain's functional connectome to link it with consciousness alterations to better comprehend how resulting neural and phenomenological changes are interconnected. Overall, we found that psilocybin administration led to a tendency of the brain to recurrently configure in a globally hyperconnected pattern, which was linked to heightened reports of OBN (experience of unity, blissfulness, insightfulness, and spiritual experience) and VRS (complex imagery, elementary imagery, audio-visual synesthesia, and changed meaning of percepts).

Regarding experiential changes, the psilocybin group exhibited significant increases across all dimensions and factors compared with the placebo group, including derealization, depersonalization, loss of self-control, visual pseudohallucinations (both elementary and complex), audio-visual

Table 2. Neuroexperiential Analysis Indicating That Transitions From Pattern 1 to the Hyperconnected Pattern 3 Were Linked to Oceanic Boundlessness

Feature Space	Factor	Correlation Coefficient	*p* Value	FDR-Corrected *p* Value
Neural Space	T13	0.89	1.00×10^{-5}	1.60×10^{-4}[a]
	T23	0.44	3.07×10^{-2}	1.64×10^{-1}
	T43	0.43	1.71×10^{-3}	1.37×10^{-2}[b]
	T33	0.25	5.94×10^{-2}	1.91×10^{-1}
	T21	0.23	4.86×10^{-2}	1.91×10^{-1}
	T14	0.12	1.58×10^{-1}	4.22×10^{-1}
	T32	0.09	2.90×10^{-1}	5.80×10^{-1}
	T24	0.09	2.51×10^{-1}	5.73×10^{-1}
	T31	−0.01	5.37×10^{-1}	9.55×10^{-1}
	T44	−0.08	7.61×10^{-1}	9.92×10^{-1}
	T11	−0.09	6.61×10^{-1}	9.92×10^{-1}
	T41	−0.17	8.38×10^{-1}	9.92×10^{-1}
	T34	−0.27	9.70×10^{-1}	9.92×10^{-1}
	T22	−0.33	9.69×10^{-1}	9.92×10^{-1}
	T12	−0.34	9.84×10^{-1}	9.92×10^{-1}
	T42	−0.34	9.92×10^{-2}	9.92×10^{-1}
Phenomenological Space	OBN	0.93	2.90×10^{-3}	1.45×10^{-2}[b]
	VRS	0.74	4.29×10^{-2}	1.07×10^{-1}
	DED	0.46	2.02×10^{-1}	3.32×10^{-1}
	AUA	0.35	2.66×10^{-1}	3.32×10^{-1}
	VIR	0.11	4.54×10^{-1}	4.54×10^{-1}

Canonical correlation analysis between between-state transition probabilities and five dimensions of the 5D-ASC. The results are sorted from the highest correlation to the lowest. T indicates the probability of transition from one pattern to another.

5D-ASC, 5-Dimensional Altered States of Consciousness Rating Scale; AUA, auditory alteration; DED, dread of ego dissolution; FDR, false discovery rate; OBN, oceanic boundlessness; VIR, vigilance reduction; VRS, visionary restructuralization.

[a] $p < .05$

[b] $p < .001$

synesthesia, unity experiences, spiritual insight, bliss, and disembodiment (45), as previously reported (1). These findings demonstrate that a moderate psilocybin dose produces a distinct phenomenological pattern compared with a placebo. Previous research on psilocybin administration has also noted measurable changes in various dimensions compared with a placebo with dosages ranging from 45 to 315 μg/kg body weight (60,61). Our data are consistent with this dose-dependent phenomenological pattern associated with psilocybin consumption.

Regarding neural changes, the psilocybin group exhibited an overall increase in whole-brain FC, consistent with previous reports (37). Serotonergic psychedelics, including psilocybin, have been shown to alter the brain's functional organization, thereby promoting greater global integration with increased short-range and long-range functional connections (41,62,63). The dynamic analysis revealed a higher probability of the brain transitioning to a hyperconnected pattern under psilocybin than in the placebo group, a pattern that has been reported in other psychedelic studies (42). This hyperconnected state, previously shown to be characterized by maximal integration and minimal segregation (53), is consistent with the flattened landscape theory, in which specific connectivity patterns become less dominant under psychedelics, resulting in increased transition probabilities to the functionally nonspecific hyperconnected pattern (43,63,64).

Additionally, the hyperconnectivity pattern in the psilocybin group was associated with cortex-wide decreases in BOLD signal amplitude. Despite the ongoing debate about GS removal in denoising processes due to its reflection of various fMRI nuisance sources, we chose to retain GS in our analysis (65–69). This decision was based on our recent finding that GS can complement extracted connectivity patterns (59). Specifically, we observed that when the hyperconnected pattern coincided with high GS amplitude during wakeful rest, participants were more likely to report instances of mind blanking (59,70). Previously, the GS amplitude served as an indirect measure of general arousal levels, with higher amplitude indicating lower arousal and lower amplitude being linked to higher arousal (71–74). Similar results were observed after LSD intake, with a decrease in signal variance, which eventually leads to a decrease in GS (75). In our study, the hyperconnectivity pattern was associated with reduced GS amplitude, thereby further contributing to the understanding of the psychedelic state as mediated by high cortical arousal (76). It is important to mention that the hyperconnected pattern was sensitive to GS removal and did not show such signal configuration after the regression (Supplement), which is consistent with our previous work with this method (59).

In neuroexperiential terms, we found a significant association between higher transition probabilities into the hyperconnected pattern and the factors of OBN and VRS. OBN

entails a positive mood, insight, and unity experiences (25). Previous studies have linked positive ego dissolution and OBN to reduced hippocampal glutamate (1) and increased insight to reduced DMN within-network static FC (27). Our whole-brain dynamic analysis extends this by demonstrating that recurrent hyperconnected states after psilocybin intake can explain unity experiences, characterized by a disruption of the self-world boundary, contrasting with the hyperconnected pattern's atypical minimal segregation profile (53). We propose that unity feelings and visual pseudohallucinatory experiences under psilocybin are linked to the brain's inclination for highly integrated patterns, showcasing its capacity for diverse mental associations. This is supported by improved creative thinking dimensions (4,27) that are attributed to increased between-network FC of the DMN and the frontoparietal network (28), which resembles the hyperconnected pattern.

Three OBN factors (unity, bliss, insight) had the highest canonical correlations in our analysis, followed by VRS factors. Dimensional-level canonical correlations reinforced OBN's highest association with transition probabilities to the hyperconnected pattern. Despite serotonergic psychedelics historically being labeled as hallucinogens, our findings are consistent with psilocybin studies, which have emphasized OBN's primary role in phenomenological outcomes (4,77,78). OBN's overall importance in the psychedelic state is further supported by research showing that it is linked to increased serotonin 2A receptor binding potential (60,61), that it predicts FC changes (79), and that it is positively correlated with somatomotor network disconnection (80). Because OBN is defined as the positive valence associated with depersonalization and derealization, it is a key psychometric dimension describing ego phenomenological modifications (25,45). CCAs on both the 5D-ASC and 11-ASC show OBN and its factors having the strongest correlations with the latent variable of the neurobiological space. This may suggest OBN as the primary driver of psilocybin's experiential pattern, thereby prompting consideration of more precise terms such as egotropic over hallucinogenic when discussing its clinical relevance. This is not to suggest that the other psychometric dimensions/factors do not have importance or clinical relevance. Rather, we mean to raise a discussion about how egotropic effects of psilocybin may be overlooked as reflected in how the drug is labeled or categorized.

Our study has several limitations. First, the absence of concurrent physiological recordings during fMRI scanning restricts tracking arousal levels, leaving us to use GS amplitude as a proxy for cortical arousal. Simultaneous physiological and electrophysiological recordings in future studies could enhance the understanding of neuronal firing during hyperconnected patterns. Second, the between-participant design, which also requires brain anatomy normalization to the Montreal Neurological Institute space, could hamper the reproducibility of the findings. A proper within-participant design is required in future studies to mitigate this shortcoming. Furthermore, we recognize that, even with classic mitigations at preprocessing, the effect of motion can still influence the findings obtained. Similar effects can also come from the shift in the neurovascular coupling that occurs during psychedelics, as recent work in mice with calcium imaging has shown (81). Fourth, we are aware that due to methodological differences using an eyes-open condition during rest, our results are not fully consistent with other protocols in which the psychedelic effects were maximized with eyes closed. However, as in our previous study, we showed that the characteristic psychedelic effects could be found in this cohort of participants even in the eyes-open condition (1), so we remain assured that we also characterized this state adequately. Also, in our previous work, we identified differences in the DMN, which in the current analysis was not a straightforward finding. We believe that this discrepancy is due to the adoption of a whole-brain network characterization using an atlas-based parcellation with multiple ROIs, which can reduce the sensitivity of capturing network-level alterations. Lastly, the analysis' reliance on the recruited population may limit generalizability, although previous studies have demonstrated replicability and universality of recurrent connectivity patterns in different datasets and brain parcellations (53,59).

Conclusions

In summary, psilocybin induces significant alterations in both brain function and subjective experience, thereby promoting a functionally nonspecific hyperconnected organization. The hyperconnected state is correlated with reported experiences of OBN and visual pseudohallucinations, which highlights the complex interplay between brain dynamics and subjective phenomena that potentially reflects the ability to entertain variant mental associations. In total, these findings illuminate the intricate interplay between brain dynamics and subjective experience under psilocybin and provide insights into the neurophysiology and neuroexperiential qualities of the psychedelic state.

ACKNOWLEDGMENTS AND DISCLOSURES

This work was supported by the Fund for Scientific Research (to SM, LDF, AD), the European Union's Horizon 2020 Research and Innovation Marie Skłodowska-Curie RISE program NeuronsXnets (Grant No. 101007926 [to AD]), the European Cooperation in Science and Technology COST Action (Grant No. CA18106 [to AD]), and the Léon Fredericq Foundation (to SM, LDF, AD).

JGR and AD contributed to the conception and design of the work; NLM acquired the data; SM, and LDF contributed with data analysis; all authors contributed to data interpretation; SM, LDF, and AD drafted and revised the manuscript; all authors proofread the submitted work.

We acknowledge Dr. Camilo Miguel Signorelli for useful discussions during the paper preparation.

A previous version of this article was published as a preprint on bioRxiv: https://www.biorxiv.org/content/10.1101/2023.09.18.558309v2.

The connectomes and the accompanying covariates used to differentiate individuals can be made available to qualified research institutions upon reasonable request to JGR and a data use agreement executed with Maastricht University. All codes used for analysis are freely available at https://gitlab.uliege.be/S.Mortaheb/psychedelics.

The authors report no biomedical financial interests or potential conflicts of interest.

ARTICLE INFORMATION

From the Physiology of Cognition, GIGA Research, CRC Human Imaging Unit, University of Liège, Liège, Belgium (SM, LDF, AD); Fund for Scientific Research FNRS, Brussels, Belgium (SM, LDF, AD); Department of Neuropsychology and Psychopharmacology, Faculty of Psychology and Neuroscience, Maastricht University, Maastricht, The Netherlands (NLM, PM, JGR); and Psychology & Neuroscience of Cognition, University of Liège, Liège, Belgium (AD).

SM and LDF are joint first authors.

JGR and AD are joint last authors.

Address correspondence to Johannes G. Ramaekers, Ph.D., at j.ramaekers@maastrichtuniversity.nl, or Athena Demertzi, Ph.D., at a.demertzi@uliege.be.

Received Jan 20, 2024; revised Mar 28, 2024; accepted Apr 1, 2024.

Supplementary material cited in this article is available online at https://doi.org/10.1016/j.bpsc.2024.04.001.

REFERENCES

1. Mason NL, Kuypers KPC, Müller F, Reckweg J, Tse DHY, Toennes SW, *et al.* (2020): Me, myself, bye: Regional alterations in glutamate and the experience of ego dissolution with psilocybin. Neuropsychopharmacology 45:2003–2011.
2. Metzner R (1998): Hallucinogenic drugs and plants in psychotherapy and shamanism. J Psychoactive Drugs 30:333–341.
3. Volgin AD, Yakovlev OA, Demin KA, Alekseeva PA, Kyzar EJ, Collins C, *et al.* (2019): Understanding central nervous system effects of deliriant hallucinogenic drugs through experimental animal models. ACS Chem Neurosci 10:143–154.
4. Nichols DE (2016): Psychedelics. Pharmacol Rev 68:264–355.
5. Kwan AC, Olson DE, Preller KH, Roth BL (2022): The neural basis of psychedelic action. Nat Neurosci 25:1407–1419.
6. Moreno FA, Wiegand CB, Taitano EK, Delgado PL (2006): Safety, tolerability, and efficacy of psilocybin in 9 patients with obsessive–compulsive disorder. J Clin Psychiatry 67:1735–1740.
7. Grob CS, Danforth AL, Chopra GS, Hagerty M, McKay CR, Halberstadt AL, Greer GR (2011): Pilot study of psilocybin treatment for anxiety in patients with advanced-stage cancer. Arch Gen Psychiatry 68:71–78.
8. Andersen KAA, Carhart-Harris R, Nutt DJ, Erritzoe D (2021): Therapeutic effects of classic serotonergic psychedelics: A systematic review of modern-era clinical studies. Acta Psychiatr Scand 143:101–118.
9. Carhart-Harris RL, Giribaldi B, Watts R, Baker-Jones M, Murphy-Beiner A, Murphy R, *et al.* (2021): Trial of psilocybin versus escitalopram for Depression. N Engl J Med 384:1402–1411.
10. Carhart-Harris RL, Erritzoe D, Williams T, Stone JM, Reed LJ, Colasanti A, *et al.* (2012): Neural correlates of the psychedelic state as determined by fMRI studies with psilocybin. Proc Natl Acad Sci U S A 109:2138–2143.
11. Ross S, Bossis A, Guss J, Agin-Liebes G, Malone T, Cohen B, *et al.* (2016): Rapid and sustained symptom reduction following psilocybin treatment for anxiety and depression in patients with life-threatening cancer: A randomized controlled trial. J Psychopharmacol 30:1165–1180.
12. Carhart-Harris RL, Bolstridge M, Rucker J, Day CMJ, Erritzoe D, Kaelen M, *et al.* (2016): Psilocybin with psychological support for treatment-resistant depression: An open-label feasibility study. Lancet Psychiatry 3:619–627.
13. Carhart-Harris RL, Roseman L, Bolstridge M, Demetriou L, Pannekoek JN, Wall MB, *et al.* (2017): Psilocybin for treatment-resistant depression: fMRI-measured brain mechanisms. Sci Rep 7:13187.
14. Carhart-Harris RL, Bolstridge M, Day CMJ, Rucker J, Watts R, Erritzoe DE, *et al.* (2018): Psilocybin with psychological support for treatment-resistant depression: Six-month follow-up. Psychopharmacology 235:399–408.
15. Davis AK, Barrett FS, May DG, Cosimano MP, Sepeda ND, Johnson MW, *et al.* (2021): Effects of psilocybin-assisted therapy on major depressive disorder: A randomized clinical trial. JAMA Psychiatry 78:481–489.
16. Griffiths RR, Johnson MW, Carducci MA, Umbricht A, Richards WA, Richards BD, *et al.* (2016): Psilocybin produces substantial and sustained decreases in depression and anxiety in patients with life-threatening cancer: A randomized double-blind trial. J Psychopharmacol 30:1181–1197.
17. Anderson BT, Danforth A, Daroff PR, Stauffer C, Ekman E, Agin-Liebes G, *et al.* (2020): Psilocybin-assisted group therapy for demoralized older long-term AIDS survivor men: An open-label safety and feasibility pilot study. EClinicalmedicine 27:100538.
18. Johnson MW, Garcia-Romeu A, Griffiths RR (2017): Long-term follow-up of psilocybin-facilitated smoking cessation. Am J Drug Alcohol Abuse 43:55–60.
19. Bogenschutz MP, Forcehimes AA, Pommy JA, Wilcox CE, Barbosa PC, Strassman RJ (2015): Psilocybin-assisted treatment for alcohol dependence: A proof-of-concept study. J Psychopharmacol 29:289–299.
20. Garcia-Romeu A, Davis AK, Erowid F, Erowid E, Griffiths RR, Johnson MW (2019): Cessation and reduction in alcohol consumption and misuse after psychedelic use. J Psychopharmacol 33:1088–1101.
21. Johnson MW, Garcia-Romeu A, Cosimano MP, Griffiths RR (2014): Pilot study of the 5-HT $_{2A}$ R agonist psilocybin in the treatment of tobacco addiction. J Psychopharmacol 28:983–992.
22. Bayne T, Carter O (2018): Dimensions of consciousness and the psychedelic state. Neurosci Conscious 2018:niy008.
23. Rock AJ, Krippner S (2007): Does the concept of "altered states of consciousness" rest on a mistake? Int J Transpersonal Stud 26:33–40.
24. Nour MM, Carhart-Harris RL (2017): Psychedelics and the science of self-experience. Br J Psychiatry 210:177–179.
25. Studerus E, Gamma A, Vollenweider FX (2010): Psychometric evaluation of the altered states of consciousness rating scale (OAV). PLoS One 5:e12412.
26. Girn M, Mills C, Roseman L, Carhart-Harris RL, Christoff K (2020): Updating the dynamic framework of thought: Creativity and psychedelics. Neuroimage 213:116726.
27. Mason NL, Kuypers KPC, Reckweg JT, Müller F, Tse DHY, Da Rios B, *et al.* (2021): Spontaneous and deliberate creative cognition during and after psilocybin exposure. Transl Psychiatry 11:209.
28. Carhart-Harris RL, Leech R, Hellyer PJ, Shanahan M, Feilding A, Tagliazucchi E, *et al.* (2014): The entropic brain: A theory of conscious states informed by neuroimaging research with psychedelic drugs. Front Hum Neurosci 8:20.
29. Griffiths RR, Richards WA, McCann U, Jesse R (2006): Psilocybin can occasion mystical-type experiences having substantial and sustained personal meaning and spiritual significance. Psychopharmacology 187:268–283; discussion 284.
30. Preller KH, Vollenweider FX (2018): Phenomenology, structure, and dynamic of psychedelic states. In: Halberstadt AL, Vollenweider FX, Nichols DE, editors. Behavioral Neurobiology of Psychedelic Drugs. Berlin, Heidelberg: Springer, 221–256.
31. Majić T, Schmidt TT, Gallinat J (2015): Peak experiences and the afterglow phenomenon: When and how do therapeutic effects of hallucinogens depend on psychedelic experiences? J Psychopharmacol 29:241–253.
32. Erritzoe D, Roseman L, Nour MM, MacLean K, Kaelen M, Nutt DJ, Carhart-Harris RL (2018): Effects of psilocybin therapy on personality structure. Acta Psychiatr Scand 138:368–378.
33. MacLean KA, Johnson MW, Griffiths RR (2011): Mystical experiences occasioned by the hallucinogen psilocybin lead to increases in the personality domain of openness. J Psychopharmacol 25:1453–1461.
34. Madsen MK, Fisher PM, Stenbæk DS, Kristiansen S, Burmester D, Lehel S, *et al.* (2020): A single psilocybin dose is associated with long-term increased mindfulness, preceded by a proportional change in neocortical 5-HT2A receptor binding. Eur Neuropsychopharmacol 33:71–80.
35. Daws RE, Timmermann C, Giribaldi B, Sexton JD, Wall MB, Erritzoe D, *et al.* (2022): Increased global integration in the brain after psilocybin therapy for depression. Nat Med 28:844–851.
36. Preller KH, Duerler P, Burt JB, Ji JL, Adkinson B, Stämpfli P, *et al.* (2020): Psilocybin induces time-dependent changes in global functional connectivity. Biol Psychiatry 88:197–207.
37. Roseman L, Leech R, Feilding A, Nutt DJ, Carhart-Harris RL (2014): The effects of psilocybin and MDMA on between-network resting state functional connectivity in healthy volunteers. Front Hum Neurosci 8:204.
38. Barrett FS, Krimmel SR, Griffiths RR, Seminowicz DA, Mathur BN (2020): Psilocybin acutely alters the functional connectivity of the claustrum with brain networks that support perception, memory, and attention. Neuroimage 218:116980.

39. McCulloch DE, Madsen MK, Stenbæk DS, Kristiansen S, Ozenne B, Jensen PS, *et al.* (2022): Lasting effects of a single psilocybin dose on resting-state functional connectivity in healthy individuals. J Psychopharmacol 36:74–84.
40. Madsen MK, Stenbæk DS, Arvidsson A, Armand S, Marstrand-Joergensen MR, Johansen SS, *et al.* (2021): Psilocybin-induced changes in brain network integrity and segregation correlate with plasma psilocin level and psychedelic experience. Eur Neuropsychopharmacol 50:121–132.
41. Petri G, Expert P, Turkheimer F, Carhart-Harris R, Nutt D, Hellyer PJ, Vaccarino F (2014): Homological scaffolds of brain functional networks. J R Soc Interface 11:20140873.
42. Lord LD, Expert P, Atasoy S, Roseman L, Rapuano K, Lambiotte R, *et al.* (2019): Dynamical exploration of the repertoire of brain networks at rest is modulated by psilocybin. Neuroimage 199:127–142.
43. Singleton SP, Luppi AI, Carhart-Harris RL, Cruzat J, Roseman L, Nutt DJ, *et al.* (2022): Receptor-informed network control theory links LSD and psilocybin to a flattening of the brain's control energy landscape. Nat Commun 13:5812.
44. Olsen AS, Lykkebo-Valløe A, Ozenne B, Madsen MK, Stenbæk DS, Armand S, *et al.* (2022): Psilocybin modulation of time-varying functional connectivity is associated with plasma psilocin and subjective effects. Neuroimage 264:119716.
45. Dittrich A (1998): The standardized psychometric assessment of altered states of consciousness (ASCs) in humans. Pharmacopsychiatry 31(suppl 2):80–84.
46. Pekala RJ (2013): Quantifying Consciousness: An Empirical Approach. New York, NY: Springer Science and Business Media.
47. Penny WD, Friston KJ, Ashburner JT, Kiebel SJ, Nichols TE (2011): Statistical Parametric Mapping: The Analysis of Functional Brain Images. Amsterdam: Elsevier.
48. Jenkinson M, Beckmann CF, Behrens TEJ, Woolrich MW, Smith SM (2012): FSL. Neuroimage 62:782–790.
49. Andersson JLR, Skare S, Ashburner J (2003): How to correct susceptibility distortions in spin-echo echo-planar images: Application to diffusion tensor imaging. Neuroimage 20:870–888.
50. Gorgolewski K, Burns CD, Madison C, Clark D, Halchenko YO, Waskom ML, Ghosh SS (2011): Nipype: A flexible, lightweight and extensible neuroimaging data processing framework in Python. Front Neuroinform 5:13.
51. Schaefer A, Kong R, Gordon EM, Laumann TO, Zuo XN, Holmes AJ, *et al.* (2018): Local-global parcellation of the human cerebral cortex from intrinsic functional connectivity MRI. Cereb Cortex 28:3095–3114.
52. Barttfeld P, Uhrig L, Sitt JD, Sigman M, Jarraya B, Dehaene S (2015): Signature of consciousness in the dynamics of resting-state brain activity. Proc Natl Acad Sci U S A 112:887–892.
53. Demertzi A, Tagliazucchi E, Dehaene S, Deco G, Barttfeld P, Raimondo F, *et al.* (2019): Human consciousness is supported by dynamic complex patterns of brain signal coordination. Sci Adv 5:eaat7603.
54. Mihalik A, Chapman J, Adams RA, Winter NR, Ferreira FS, Shawe-Taylor J, *et al.* (2022): Canonical correlation analysis and partial least squares for identifying brain–behavior associations: A tutorial and a comparative study. Biol Psychiatry Cogn Neurosci Neuroimaging 7:1055–1067.
55. Power JD, Mitra A, Laumann TO, Snyder AZ, Schlaggar BL, Petersen SE (2014): Methods to detect, characterize, and remove motion artifact in resting state fMRI. Neuroimage 84:320–341.
56. Griffa A, Amico E, Liégeois R, Van De Ville D, Preti MG (2022): Brain structure-function coupling provides signatures for task decoding and individual fingerprinting. Neuroimage 250:118970.
57. Glasser MF, Sotiropoulos SN, Wilson JA, Coalson TS, Fischl B, Andersson JL, *et al.* (2013): The minimal preprocessing pipelines for the Human Connectome Project. Neuroimage 80: 105–124.
58. Fischl B, Salat DH, Busa E, Albert M, Dieterich M, Haselgrove C, *et al.* (2002): Whole brain segmentation: Automated labeling of neuroanatomical structures in the human brain. Neuron 33:341–355.
59. Mortaheb S, Van Calster L, Raimondo F, Klados MA, Boulakis PA, Georgoula K, *et al.* (2022): Mind blanking is a distinct mental state linked to a recurrent brain profile of globally positive connectivity during ongoing mentation. Proc Natl Acad Sci U S A 119:e2200511119.
60. Hasler F, Grimberg U, Benz MA, Huber T, Vollenweider FX (2004): Acute psychological and physiological effects of psilocybin in healthy humans: A double-blind, placebo-controlled dose-effect study. Psychopharmacology 172:145–156.
61. Quednow BB, Kometer M, Geyer MA, Vollenweider FX (2012): Psilocybin-Induced Deficits in Automatic and Controlled Inhibition are Attenuated by ketanserin in Healthy Human Volunteers. Neuropsychopharmacology 37:630–640.
62. Tagliazucchi E, Roseman L, Kaelen M, Orban C, Muthukumaraswamy SD, Murphy K, *et al.* (2016): Increased global functional connectivity correlates with LSD-induced ego dissolution. Curr Biol 26:1043–1050.
63. Timmermann C, Roseman L, Haridas S, Rosas FE, Luan L, Kettner H, *et al.* (2023): Human brain effects of DMT assessed via EEG-fMRI. Proc Natl Acad Sci U S A 120:e2218949120.
64. Carhart-Harris RL, Friston KJ (2019): REBUS and the anarchic brain: Toward a Unified Model of the brain action of psychedelics. , editor. Pharmacol Rev Barker EL 71:316–344.
65. Murphy K, Fox MD (2017): Towards a consensus regarding global signal regression for resting state functional connectivity MRI. Neuroimage 154:169–173.
66. Power JD, Plitt M, Laumann TO, Martin A (2017): Sources and implications of whole-brain fMRI signals in humans. Neuroimage 146:609–625.
67. Chang C, Glover GH (2010): Time–frequency dynamics of resting-state brain connectivity measured with fMRI. Neuroimage 50:81–98.
68. Zhu DC, Tarumi T, Khan MA, Zhang R (2015): Vascular coupling in resting-state FMRI: Evidence from multiple modalities. J Cereb Blood Flow Metab 35:1910–1920.
69. Colenbier N, Van de Steen F, Uddin LQ, Poldrack RA, Calhoun VD, Marinazzo D (2020): Disambiguating the role of blood flow and global signal with partial information decomposition. Neuroimage 213:116699.
70. Ward AF, Wegner DM (2013): Mind-blanking: When the mind goes away. Front Psychol 4:650.
71. Fukunaga M, Horovitz SG, Van Gelderen P, De Zwart JA, Jansma JM, Ikonomidou VN, *et al.* (2006): Large-amplitude, spatially correlated fluctuations in BOLD fMRI signals during extended rest and early sleep stages. Magn Reson Imaging 24:979–992.
72. Nilsonne G, Tamm S, Schwarz J, Almeida R, Fischer H, Kecklund G, *et al.* (2017): Intrinsic brain connectivity after partial sleep deprivation in young and older adults: Results from the Stockholm Sleepy Brain study. Sci Rep 7:9422.
73. Wong CW, Olafsson V, Tal O, Liu TT (2013): The amplitude of the resting-state fMRI global signal is related to EEG vigilance measures. Neuroimage 83:983–990.
74. Liu X, de Zwart JA, Schölvinck ML, Chang C, Ye FQ, Leopold DA, Duyn JH (2018): Subcortical evidence for a contribution of arousal to fMRI studies of brain activity. Nat Commun 9:395.
75. Carhart-Harris RL, Muthukumaraswamy S, Roseman L, Kaelen M, Droog W, Murphy K, *et al.* (2016): Neural correlates of the LSD experience revealed by multimodal neuroimaging. Proc Natl Acad Sci U S A 113:4853–4858.
76. Carhart-Harris RL, Leech R, Erritzoe D, Williams TM, Stone JM, Evans J, *et al.* (2013): Functional connectivity measures after psilocybin inform a novel hypothesis of early psychosis. Schizophr Bull 39:1343–1351.
77. Metzner R (2005): Psychedelic, psychoactive, and addictive drugs and states of consciousness. In: Mind-Altering Drugs: The Science of Subjective Experience. New York: Oxford University Press. Available at: http://archive.org/details/mindalteringdrug0000unse. Accessed August 30, 2023.

78. von Rotz R, Schindowski EM, Jungwirth J, Schuldt A, Rieser NM, Zahoranszky K, *et al.* (2023): Single-dose psilocybin-assisted therapy in major depressive disorder: A placebo-controlled, double-blind, randomised clinical trial. EClinicalmedicine 56:101809.
79. Smigielski L, Scheidegger M, Kometer M, Vollenweider FX (2019): Psilocybin-assisted mindfulness training modulates self-consciousness and brain default mode network connectivity with lasting effects. Neuroimage 196:207–215.
80. Preller KH, Burt JB, Ji JL, Schleifer CH, Adkinson BD, Stämpfli P, *et al.* (2018): Changes in global and thalamic brain connectivity in LSD-induced altered states of consciousness are attributable to the 5-HT2A receptor. eLife 7:e35082.
81. Padawer-Curry JA, Snyder AZ, Bice AR, Wang X, Nicol GE, McCall JG, *et al.* (2023): Psychedelic 5-HT2A receptor agonism: Neuronal signatures and altered neurovascular coupling. bioRxiv. https://doi.org/10.1101/2023.09.23.559145.